

WenLan 2.0: Make AI Imagine via a Multimodal Foundation Model

Nanyi Fei^{2,3}, Zhiwu Lu^{1,2}, Yizhao Gao^{1,2}, Guoxing Yang^{1,2}, Yuqi Huo^{2,3}, Jingyuan Wen^{1,2},
Haoyu Lu^{1,2}, Ruihua Song^{1,2}, Xin Gao⁴, Tao Xiang⁵, Hao Sun^{1,2,6} and Ji-Rong Wen^{1,2,3}

¹*Gaoling School of Artificial Intelligence, Renmin University of China, Beijing, China*

²*Beijing Key Laboratory of Big Data Management and Analysis Methods, Beijing, China*

³*School of Information, Renmin University of China, Beijing, China*

⁴*Computer, Electrical and Mathematical Sciences and Engineering Division, King Abdullah University of Science and Technology, Thuwal, Saudi Arabia*

⁵*Department of Electrical and Electronic Engineering, University of Surrey, Guildford, United Kingdom*

⁶*Department of Civil and Environmental Engineering, Massachusetts Institute of Technology, Cambridge, USA*

Abstract— The fundamental goal of artificial intelligence (AI) is to mimic the core cognitive activities of human including perception, memory, and reasoning. Although tremendous success has been achieved in various AI research fields (e.g., computer vision and natural language processing), the majority of existing works only focus on acquiring single cognitive ability (e.g., image classification, reading comprehension, or visual commonsense reasoning). To overcome this limitation and take a solid step to artificial general intelligence (AGI), we develop a novel foundation model pre-trained with huge multimodal (visual and textual) data, which is able to be quickly adapted for a broad class of downstream cognitive tasks. Such a model is fundamentally different from the multimodal foundation models recently proposed in the literature that typically make strong semantic correlation assumption and expect exact alignment between image and text modalities in their pre-training data, which is often hard to satisfy in practice thus limiting their generalization abilities. To resolve this issue, we propose to pre-train our foundation model by self-supervised learning with weak semantic correlation data crawled from the Internet and show that state-of-the-art results can be obtained on a wide range of downstream tasks (both single-modal and cross-modal). Particularly, with novel model-interpretability tools developed in this work, we demonstrate that strong imagination ability (even with hints of commonsense) is now possessed by our foundation model. We believe our work makes a transformative stride towards AGI and will have broad impact on various AI+ fields (e.g., neuroscience and healthcare).

Introduction

Science fictions and sci-fi films, that describe highly intelligent computer minds, robots, or even human-shaped ones, can be said to understand or have primitive cognitive abilities analogous to human intelligence. Since this ultimate form of human-level artificial intelligence (AI) is extremely far from reality hitherto, researchers change to set a less ambitious goal of achieving artificial general intelligence (AGI). Despite not being precisely defined, AGI is broadly agreed to have several key features [1] including: (1) matching or exceeding human performance across a broad class of cognitive tasks (e.g., perception, reading comprehension, and reasoning) in a variety of contexts and environments; (2) possessing the ability to handle problems quite different from those anticipated by its creators; and (3) being able to generalize/transfer the learned knowledge from one context to others. As we can imagine, devising and obtaining an AGI system would not only accelerate the AI research itself, but also benefit a wide range of AI+ fields including neuroscience, healthcare, and biomedicine.

In recent years, deep learning [2] has achieved tremendous successes in various AI research areas such as computer vision (CV) and natural language processing (NLP). For example, deep residual networks (ResNets) [3] have already surpassed human performance on image classification. The language model RoBERTa [4] has also outperformed human on several natural language understanding tasks of the GLUE benchmark [5]. Relation networks [6] devised by DeepMind have achieved super-human performance on a relational reasoning dataset. However, most of existing AI advances only focus on approaching or exceeding human intelligence on single cognitive ability (e.g., image classification, language understanding, or relational reasoning). To overcome such a limitation and take a solid step to AGI, we develop a foundation model pre-trained with huge multimodal (visual and textual) data such that it can be quickly adapted for a broad class of downstream cognitive tasks.

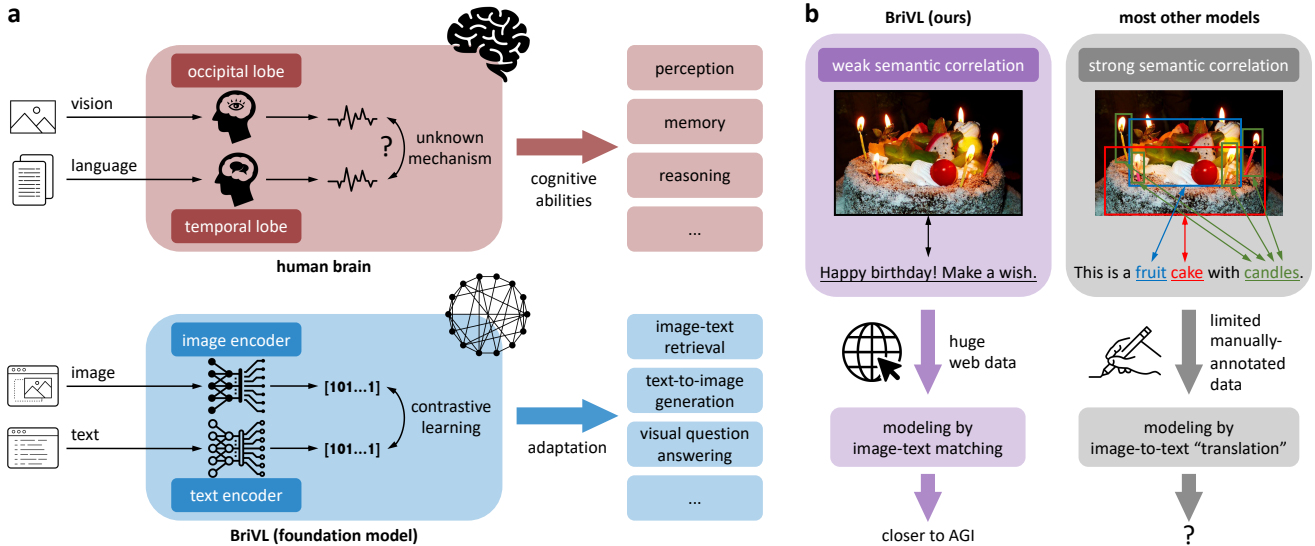


Fig. 1: **Overarching concept of our BriVL model with weak training data assumption.** **a.** Comparison between the human brain and our multimodal foundation model BriVL (**B**ridging-**V**ision-and-**L**anguage) for coping with both vision and language information. **b.** Comparison between modeling weak semantic correlation data and modeling strong semantic correlation data.

Our motivations are two-fold: (1) Foundation models [7] (also well-known as pre-trained models) are established because they are exactly designed to be adapted (e.g., finetuned) to various downstream cognitive tasks by pre-training on broad data at scale. Importantly, foundation models are closely related to two breakthroughs of MIT Technology Review’s “10 Breakthrough Technologies 2021”¹: GPT-3 [8] (a pre-trained language model) and multi-skilled AI. (2) Our choice of learning from huge multimodal data is inspired by the fact that most human intelligent behaviors are exhibited in a multimodal context using visual-textual content as the primary carrier of knowledge and means of communication (see Fig. 1a). Indeed, researchers have reported that a subset of neurons in the human medial temporal lobe can be selectively activated by representations of a specific object/scene across different sensory modalities (e.g., pictures, written names, and spoken names) [9, 10]. Although the mechanism of cross-modal alignment in our brain is unknown, this still suggests that human brain neurons are able to process multimodal information and encode concepts into invariant representations. Overall, we believe that pre-training a large-scale *multimodal foundation* model is indeed a potential approach to achieving AGI.

Multimodal (visual and textual) foundation models [11, 12] typically take image-text pairs as input and model the correlation between two different modalities in their pre-training data. Although existing multimodal foundation models have shown promising results on fast learning/transfer and cross-modal understanding tasks, the majority of them [11, 13–17] make the assumption of strong semantic correlation over the input image-text pairs (e.g., image-caption pairs) and expect exact matches between the objects/regions in an image and the words in a piece of text (see Fig. 1b). This seriously limits these models’ generalization abilities because the strong semantic correlation assumption is often invalid in the real world and multimodal data following this assumption is limited (e.g., only millions of image-caption pairs are collected by years of human annotation). This situation becomes worse when latest multimodal foundation models [11, 16, 18–20] often employ object detectors to obtain meaningful image regions and adopt a single-tower network architecture for better modeling the fine-grained region-word matching (i.e., taking the concatenation of image regions and text words as input). These two common practices (i.e., object detectors and single-tower architecture) are both computationally costly and thus unsuited for real-world applications. Particularly, as for the latter, given a query in cross-modal retrieval (text-to-image or image-to-text), all possible query-candidate pairs need to be fed into the model to compute matching scores, resulting in large latency in retrieval.

To address the above issues, we develop a novel large-scale multimodal foundation model dubbed **B**ridging-**V**ision-and-**L**anguage (BriVL) by self-supervised learning [21–24] from huge multimodal data. Firstly, to build our pre-training data collection, we choose to exploit weak semantic correlation data (see Fig. 1b) available on the Internet without any need of human annotation (i.e., we crawl a total of 650 million image-text pairs from the web). Importantly, such huge weak semantic correlation data contains complicated/abstract human emotions and thoughts. Therefore, comparing to modeling strong semantic correlation data by direct image-to-text “translation” in previous works [11, 16, 18–20], modeling weak semantic correlation data by image-text matching would help us obtain a more cognitive model. Secondly, to design our network architecture, since there do not necessarily exist fine-grained region-word matches

¹<https://www.technologyreview.com/2021/02/24/1014369/10-breakthrough-technologies-2021/>

between image and text modalities, we drop the time-consuming object detectors and adopt a simple two-tower architecture (instead of the single-tower one), which encodes image and text inputs using two separate encoders (see Fig. 1a). Note that the two-tower architecture has a clear advantage in efficiency during inference, as the embeddings of candidates can be computed and indexed before querying, meeting the latency requirement of real-world applications. Thirdly, with the advancement of large-scale distributed training techniques [25, 26] and self-supervised learning [21–24], learning from *huge unannotated* multimodal data becomes possible. Specifically, to model the weak image-text correlation and learn a unified semantic space where global-level image/text embeddings are aligned, we devise a cross-modal contrastive learning (CL) algorithm, where CL is a special form of self-supervised learning that is initially developed in single-modality (i.e., images) [27–30] with the learning objective of keeping the positive samples close and pushing away the negative ones. The proposed network and algorithm designs are detailed in Methods.

Although OpenAI CLIP [12] and Google ALIGN [31] are most closely related to our BriVL, there exist two main differences between BriVL and these two latest models: (1) We follow the weak semantic correlation assumption and construct a huge dataset crawled from the Internet, and only pornographic/sensitive data are filtered out in our collected dataset. In contrast, CLIP only keeps image-text pairs with high word frequency (i.e., the long-tail concepts are discarded), while ALIGN also filters its pre-training dataset by some rules (e.g., excluding texts shared by more than 10 images, excluding texts with extremely low word frequency, and excluding texts that are too long or too short). Our dataset thus preserves a data distribution closer to that of the real world. (2) Inspired by the single-modal contrastive learning (CL) algorithm MoCo [28], our BriVL model adopts a momentum mechanism to dynamically maintain queues of negative samples across different training batches. In this way, we have a large negative sample size (crucial for CL) while using a relatively small batch size (to reduce GPU memory footprint). On the contrary, both CLIP and ALIGN use negative samples within each training batch, requiring a large batch size (i.e., a great demand for GPU memories/resources). More technical differences can be found in Methods.

We conduct extensive experiments on various downstream cognitive tasks (e.g., news classification in single-modal and visual question answering in cross-modal) and show that our foundation model BriVL achieves state-of-the-art results, demonstrating its cross-modal understanding ability and cross-domain learning/transfer ability. Although our BriVL is only pre-trained with an image-text matching learning objective, its strong generalization ability has already satisfied some of the key features that an AGI system should have. Importantly, our foundation model even exhibits the commonsense understanding ability. A closer examination reveals that this is mainly due to the fact that our BriVL leverages weak semantic correlation data in large-scale multimodal pre-training. Moreover, with a couple of novel model-interpretability tools developed in this work, we show that strong imagination ability (even with hints of commonsense) is now possessed by our BriVL. To the best of our knowledge, this is the first time in the literature that we manage to visually reveal how a multimodal foundation model understands language (e.g., words and sentences). Overall, these findings indicate that pre-training a multimodal (visual and textual) foundation model can make a giant stride towards AGI. With more sensory modalities exploited for multimodal pre-training and further exploration on more advancing foundation models, we believe that we are approaching AGI and our work will have a broad impact on a variety of AI+ fields including neuroscience, healthcare, and biomedicine.

Results

Pre-Training Data Collection. We construct a huge web-crawled multi-source image-text dataset called weak semantic correlation dataset (WSCD) as our pre-training data collection. WSCD collects Chinese image-text pairs from multiple sources on the web, including news, encyclopedia, and social media. Concretely, images from these data sources, together with their corresponding/surrounding text descriptions, are used to form image-text pairs. Since the obtained image-text pairs are crawled from the web, the image and the text of each pair are expected to be weakly correlated. For example, an image from social media that contains people having a good time with friends tends to have a simple title of “What a nice day!”, without any finer-grained description of the image content. Note that we only filter out the pornographic/sensitive data from WSCD, without any form of editing/modification to the raw data to preserve the natural data distribution. Totally, WSCD has around 650 million image-text pairs covering a wide range of topics such as sports, lifestyle, and movie posters. Since WSCD is based on Chinese, English texts of all experiments in this section are translated into Chinese for our BriVL. Furthermore, we pre-train our BriVL on an English dataset and show results on English tasks in Supplementary Note Fig. S3, indicating that our foundation model also provides a feasible solution closer to AGI beyond specific languages.

Neural Network Visualization. Once BriVL is pre-trained (see Methods), we are fascinated by what exactly it has learned from such a vast amount of loosely aligned image-text pairs. Instead of examining it indirectly through downstream tasks, we extend Feature Visualization (FeaVis) [32] to see the visual responses of BriVL to semantic inputs directly. FeaVis is an algorithm designed only to visualize the features of convolutional neural networks (CNNs). However, given a large-scale cross-modal foundation model like our BriVL, we can visualize any text input by using

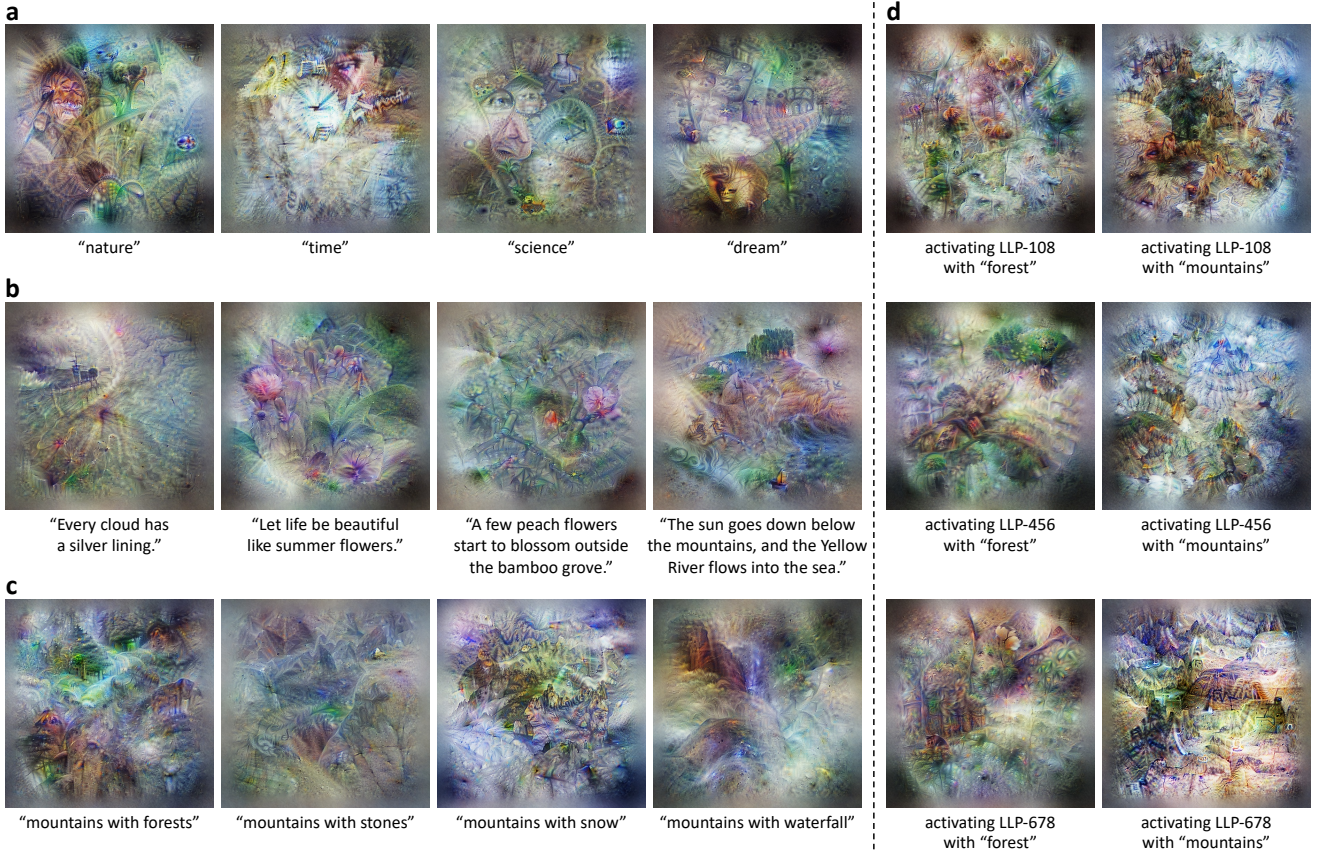


Fig. 2: **Network and neuron visualizations of our BriVL.** **a.** Visualizations of the final embedding layer of BriVL w.r.t. different high-level concepts. **b.** Visualizations of the final embedding layer of BriVL w.r.t. free-form text inputs. **c.** Visualizations of the final embedding layer of BriVL with different semantic restrictions related to “mountains with”. **d.** Visualizations for different neurons of BriVL with semantic restrictions “forest” and “mountains”.

the joint image-text embedding space as the bridge. Concretely, we first input a piece of text and obtain its text embedding through the text encoder of BriVL. Next, we randomly initialize a noisy image and also get an image embedding through the image encoder. Since the input image is randomly initialized, its embedding does not match that of the input text. We thus define the objective of matching the two embeddings and back-propagate the resultant gradients to update the input image. Note that we do not use any additional module or data for visualization, while the pre-trained BriVL is frozen during the whole process. The finally obtained image thus depicts a clear picture of what BriVL knows about the input text. The visualizations of different semantic inputs are shown in Fig. 2. Note that the input texts are originally in Chinese and translated into English for illustration purpose.

We first present the visual responses of BriVL to high-level concepts in Fig. 2a. It can be seen that, even though these concepts are rather abstract, the visualizations are able to show concrete embodiment of these concepts (e.g., “nature”: plants like grass; “time”: a clock; “science”: a face with glasses and a conical flask; “dream”: cloud, a bridge leading to a door, and the dream-like atmosphere). This ability to generalize an abstract concept to a series of more concrete objects is a sign of learned common sense and an indication of the effectiveness of our multimodal pre-training using only weak semantic correlation data (which expose the model with abstract concepts).

In Fig. 2b, we show the visualizations of sentences. The visualization of “Every cloud has a silver lining.” not only embodies the sunlight behind dark clouds literally, but also seems to show a dangerous situation on the sea (the ship-like object and the waves on the left), expressing the implicit meaning of this sentence. In the visualization of “Let life be beautiful like summer flowers.”, we can see a flower shrub. The next two text inputs describing more complicated scenes are both from ancient Chinese poems written with completely different grammar from most other texts in the dataset. It seems that BriVL also understands them well: for “A few peach flowers start to blossom outside the bamboo grove.”, there are bamboos and pink flowers; for “The sun goes down below the mountains, and the Yellow River flows into the sea.”, we can see mountains with trees hiding the sunset, and a small boat on the river. Overall, we find that BriVL possesses strong capability of imagination given a complicated sentence as prompt.

In Fig. 2c, a few similar text inputs containing a shared prompt are used for network visualization. For “mountains with forests”, there is more green area in the image; for “mountains with stones”, the image is more rocky; for “mountains with snow”, the ground turns into white/blue around the trees in the center; for “mountains with waterfall”,

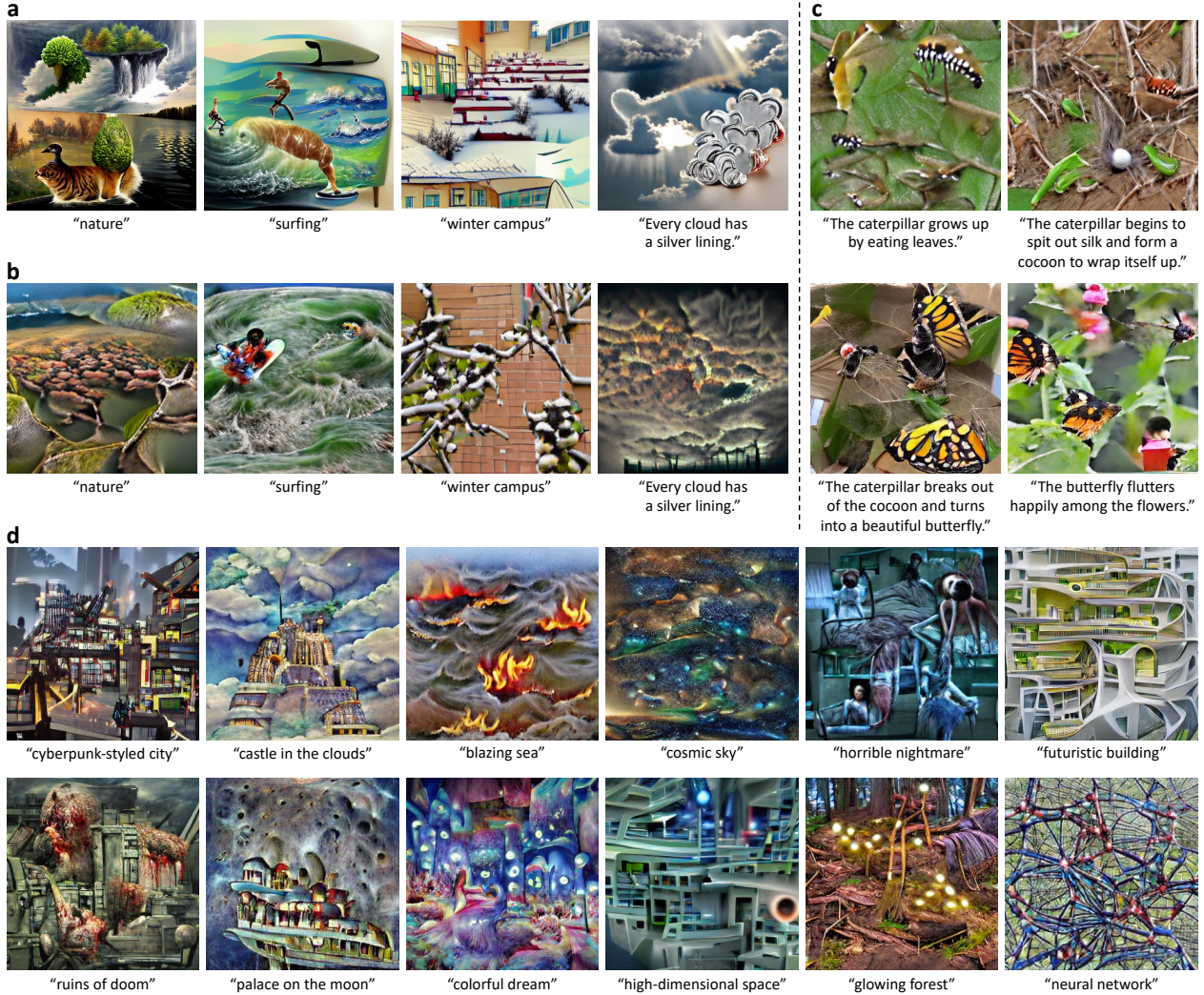


Fig. 3: **Text-to-image generation examples.** **a.** Generation examples of VQGAN inversion with CLIP (w/ ResNet-50x4). **b.** Generation examples of VQGAN inversion with our BriVL. **c.** A series of generation examples by VQGAN inversion with our BriVL. **d.** More generation examples by VQGAN inversion with our BriVL, where concepts/scenes are rarely seen by us humans (e.g., “blazing sea” and “glowing forest”) or even do not exist in real life (e.g., “cyberpunk-styled city” and “castle in the clouds”). Note that VQGAN is pre-trained on ILSVRC-2012. BriVL, CLIP and VQGAN are all frozen during text-to-image generation.

we can see blue water falling down with even vapor visible. These visualization results indicate that our model is capable of linking specific objects with more general visual context.

We also present the neuron visualization results with semantic constraints in Fig. 2d. Concretely, in addition to the image-text matching loss described above, we select neurons (i.e., channels) in the feature map of the last layer before the pooling layer (LLP, short for “Last Layer before Pooling”) in our image encoder and maximize the value of each neuron. Since each text input may contain many semantic contents, we can see what it is equivalent to activating one neuron under certain semantic constraint. Three neurons LLP-108, LLP-456, and LLP-678 (the number means the position of each channel in the feature map) are selected for neuron visualization. The two columns in Fig. 2d show the visualizations with text inputs “forest” and “mountains”, respectively. We can clearly see that even with the same semantic constraint, maximizing different neurons leads to different visualization results, indicating that each text input has rich semantics with different aspects being captured by different neurons.

Text-to-Image Generation. Network/neuron visualizations are straightforward but sometimes can be hard to interpret. In this subsection, another visualization/interpretability method is developed. Specifically, we utilize VQGAN [33] to generate images under the guidance of our BriVL and contrast them with those generated with CLIP [12]. A VQGAN pre-trained on the ILSVRC-2012 [34] dataset is excellent in generating photorealistic images given a sequence of tokens. Each of such token is a vector from the pre-trained token set (i.e., codebook) of VQGAN. We first randomly sample a sequence of tokens, and obtain a generated image from the pre-trained VQGAN. Next, we input

the generated image into the image encoder of CLIP/BriVL and also input a piece of text into the text encoder. Finally, we define the objective of matching the image and text embeddings, and back-propagate the resultant gradients to update the initial token sequence. Like network/neuron visualization, both VQGAN and CLIP/BriVL are frozen during the generation process. The generated examples are presented in Fig. 3.

In Fig. 3a and Fig. 3b, we select four text inputs and show the results obtained by CLIP and our BriVL, respectively. CLIP and BriVL both understand the texts well; however, we also observe two major differences. Firstly, cartoon-styled elements tend to appear in the generated images of CLIP, while images generated by our BriVL are more real and natural. Secondly, CLIP tends to simply put elements together while BriVL-generated images are more coherent globally. The first difference may be due to the differences in the training data used by CLIP and BriVL. The images in our training data are crawled from the Internet (most are real photos), while there may be a fair amount of cartoon images in the training data of CLIP. The second difference lies in the fact that CLIP uses image-text pairs with strong semantic correlation (by word filtering) while we use weakly correlated data. This means that during multimodal pre-training, CLIP is more likely to learn the correspondence between objects (in images) and words (in texts) while BriVL is trying to understand each image with the given text as a whole.

In Fig. 3c, we consider a significantly more challenging task where a series of images should be generated according to multiple coherent sentences. Although each image in Fig. 3c is generated independently, we can observe that all four generated images are visually coherent and of the same style. This finding demonstrates another advantage of our BriVL model: although the environment and background in an image are hard to explicitly mention in the associated text, they are not neglected in our large-scale multimodal pre-training.

We present more text-to-image generation examples obtained by VQGAN inversion with our BriVL in Fig. 3d. The text inputs are also translated from Chinese into English for presentation purpose. We choose concepts/scenes rarely seen by us humans (e.g., “blazing sea” and “glowing forest”) or even those not existing in real life (e.g., “cyberpunk-styled city” and “castle in the clouds”). We find that our proposed model can generate images quite consistent with our imagination about the input concepts/scenes, indicating its strong generalization/imagination ability. This also provides evidence that the superior performance of BriVL is not due to overfitting the pre-training data since the text inputs here correspond to concepts/scenes that even do not exist in real life. In addition, these generation examples again demonstrate the advantage of pre-training BriVL on weak semantic correlation data (otherwise the fine-grained region-word matching would harm the imagination ability of BriVL).

Remote Sensing Scene Classification. To show the cross-domain knowledge transfer ability of our pre-trained BriVL, we conduct zero-shot experiments on two remote sensing scene classification benchmarks. The first dataset is UC Merced Land-Use (UCM) [35], which has 21 classes and 100 images for each class. The size of each image in UCM is 256×256 . The second dataset is AID [36], which has 30 classes and 10,000 images in total. The size of each image in AID is 600×600 . AID is a multi-source dataset, which makes it more challenging for scene classification than the single-source UCM. Concretely, images of each class in AID are extracted from different countries and regions around the world, and also at different times and seasons of the year under different imaging conditions. This leads to larger intra-class data diversity in AID. For each dataset, we first obtain class embeddings by inputting class names into the text encoder of CLIP/BriVL. Then for each test image, we obtain its image embedding via the image encoder of CLIP/BriVL, and compute its cosine similarity with each class embedding to predict the class that it belongs to. Note that since the class names of these two datasets are all English, we need to translate them into Chinese to fit our BriVL (but the original class names are directly used for CLIP).

In the field of zero-shot learning (ZSL) [37], datasets typically follow the split of unseen and seen classes. Conventional ZSL models are thus trained with seen class data and evaluated on unseen class data. Although we do not need to train on seen classes, we still follow the common practice and split each dataset with different unseen/seen class ratios (the seen classes are simply not used). Under the split settings where the number of seen classes are not zero, we randomly sample 25 splits and report the standard deviations in brackets along with average accuracy.

The zero-shot classification results on UCM are shown in the table of Fig. 4a. Our BriVL is compared to a strong baseline ZSSC [38] specially designed for zero-shot remote sensing scene classification, and also CLIP with different CNN backbones. We can see that large-scale cross-modal foundation models achieve far higher rates compared with ZSSC, indicating their strong cross-domain knowledge transfer abilities. Moreover, our classification rates are also higher than those of all CLIP models with different CNNs, which is impressive considering the loss in English-to-Chinese translation and also cultural differences (CLIP is trained on English data while we use data crawled from Chinese Internet). Results on another dataset AID are shown in the table of Fig. 4b. Since we did not find methods conducting ZSL experiments on AID, we only make comparisons with CLIP variations. As we have mentioned, AID is more challenging than UCM, which is also reflected by the much worse performance of CLIP variations on AID than on UCM. However, our BriVL achieves similar performance on the two datasets when evaluated over all data, and the gap between BriVL and CLIP is larger on AID than that on UCM. This means that BriVL has stronger generalization ability and can cope with more complicated situations.

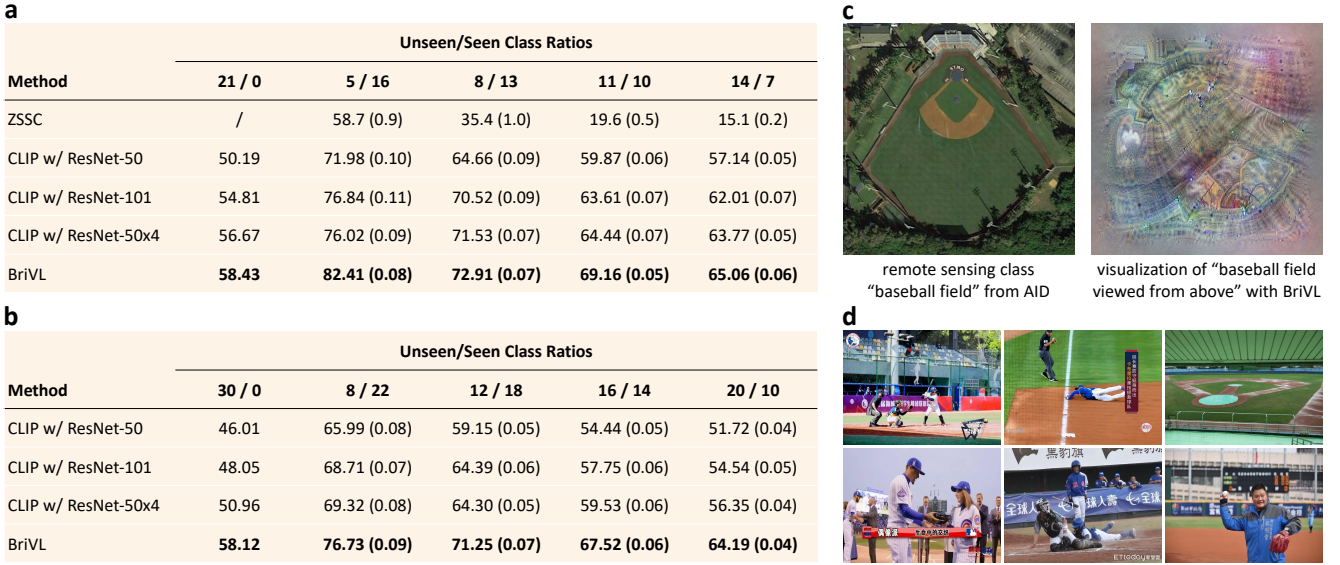


Fig. 4: **Zero-shot remote sensing scene classification results.** **a.** Zero-shot classification accuracies (%) on UCM with different unseen/seen class ratios. **b.** Zero-shot classification accuracies (%) on AID with different unseen/seen class ratios. **c.** Visualizations of “baseball field”. **d.** Image examples whose paired texts contain “baseball field” from our WSCD. For **a** and **b**, we report standard deviations in brackets over 25 random splits.

Furthermore, we deploy the network visualization technique mentioned above to clarify the visual responses of our BriVL to remote sensing related concepts. Concretely, we select one class “baseball field”, and add the prompt “viewed from above” to the class name as the text input. The visualization is shown in Fig. 4c along with one original example of this class taken from AID. We can see that remote sensing scenes are very different from the traditional photos, mainly in the perspective of cameras. Despite this, we can observe from our visualization that there is a small sector-shaped area in “baseball field viewed from above”. This provides direct explanation to the impressive performance of our BriVL on remote sensing scene classification. In addition, we search the keyword “baseball field” in our pre-training dataset WSCD and give six image examples in Fig. 4d (note that there also exist images not related to “baseball field” though their paired texts contain this keyword). We can see that these pictures are all taken in a normal camera perspective. Given that there is hardly any remote sensing data in our WSCD, these results suggest that BriVL has somehow learned to generalize transformation of perspectives to unseen domains during pre-training. This again shows the hints of common sense understanding and reasoning ability of our BriVL.

News Classification. Here we aim to demonstrate how large-scale multimodal learning can benefit single-modal learning tasks. To this end, we conduct zero-shot experiments on two Chinese news classification datasets. The first dataset is Toutiao News², which has 15 classes and a total of around 380K samples. The second dataset is THUCNews [39], which has 14 classes and around 840K samples in total. Since the contents are all texts, we only need the text encoder of our BriVL. Concretely, we first obtain class embeddings by inputting class names into the text encoder. Then for each piece of news, we only use its title to obtain its embedding via the text encoder. Finally, we compute the cosine similarities between each title embedding and class embeddings to make predictions.

The following methods are chosen for comparison: (1) RoBERTa-base [40]: it is an off-the-shelf Chinese language model pre-trained by the original authors on a large Chinese dataset with a total of 5.4B words. (2) RoBERTa-base (finetune): we finetune the pre-trained RoBERTa-base on a subset of our WSCD dataset (i.e., only the text data of 22M image-text pairs is used). (3) BriVL w/ RoBERTa-base: it is a small version of our standard BriVL since we reduce the CNN from EfficientNet-B7 [41] to EfficientNet-B5 and also the text backbone from RoBERTa-large to RoBERTa-base. We pre-train this small version with the aforementioned 22M image-text pairs. (4) RoBERTa-large: it is the larger version of RoBERTa-base and is also pre-trained by the original authors. Its pre-training data is the same as that of RoBERTa-base. (5) BriVL w/ RoBERTa-large: our standard BriVL pre-trained on the whole WSCD.

The zero-shot classification results on Toutiao News and THUCNews are shown in Fig. 5a. It can be seen that: (1) The results of RoBERTa-base are lower than those of RoBERTa-large, which is expected since the latter has more parameters and a larger model capacity. (2) On both datasets, RoBERTa-base (finetune) has limited performance gains over RoBERTa-base, while BriVL w/ RoBERTa-base outperforms RoBERTa-base by large margins. This clearly indicates the advantage of cross-modal learning over single-modal learning, given that the finetuning data of RoBERTa-

²<https://github.com/aceimnorstuvwxyz/toutiao-text-classification-dataset>

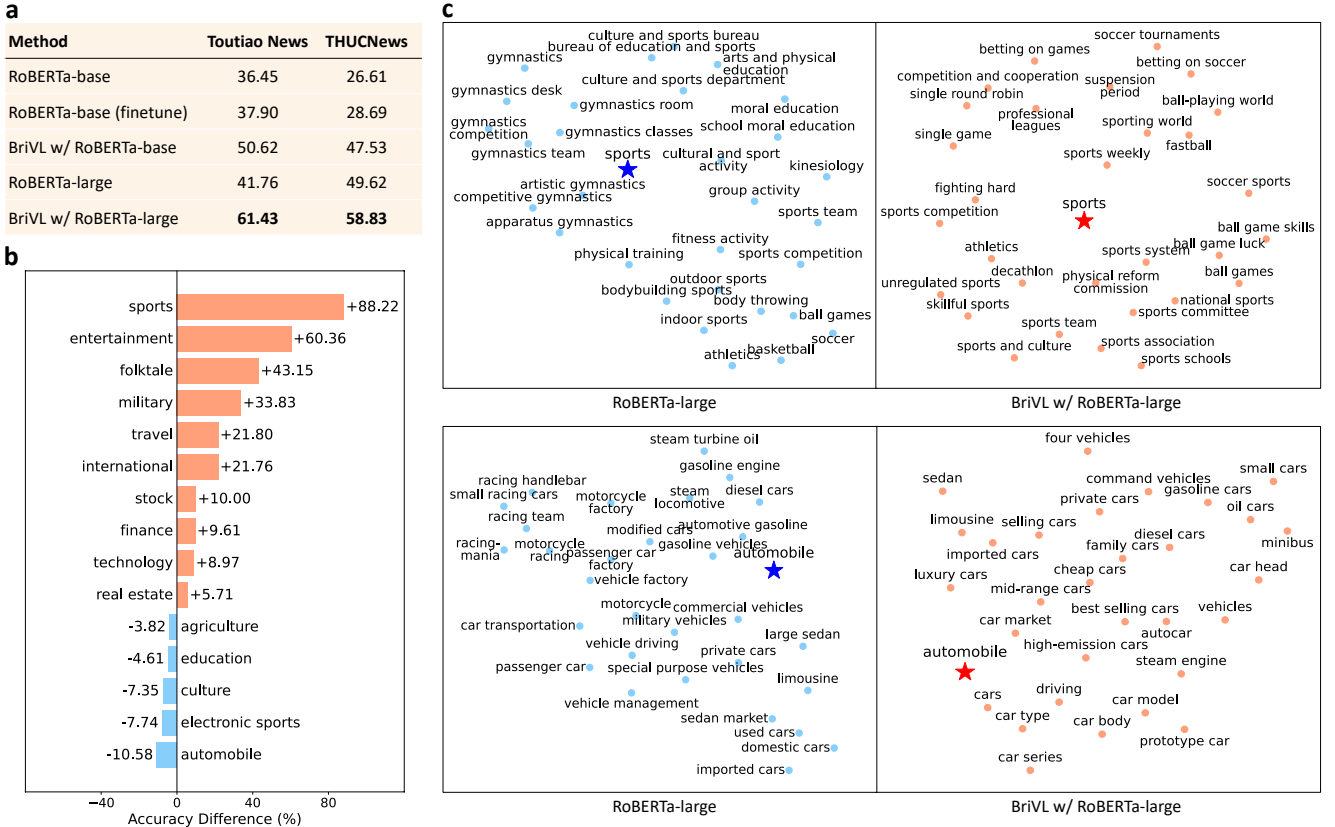


Fig. 5: **Zero-shot news classification results.** **a.** Zero-shot news classification results (%) on two Chinese news datasets. **b.** Zero-shot accuracy gain/loss (%) of BriVL w/ RoBERTa-large comparing to RoBERTa-large on each category of Toutiao News. **c.** Top-30 phrase retrieval results of “sports” (top) and “automobile” (bottom) using RoBERTa-large and BriVL w/ RoBERTa-large, respectively. The candidate phrase list is obtained from Jieba, which consists of 347,728 Chinese phrases. We translate the results into English for presentation clarity.

base (finetune) and BriVL w/ RoBERTa-base is both from the 22M subset of WSCD. (3) When it comes to RoBERTa-large, our BriVL w/ RoBERTa-large also leads to much better results than RoBERTa-large.

Moreover, in Fig. 5b, we present the performance gain/loss of our BriVL w/ RoBERTa-large comparing to RoBERTa-large on each category of Toutiao News. We can observe that the performance of BriVL decreases only on 5 categories but increases on the other 10 categories. Further, we show top-30 phrase retrieval results of the category names “sports” and “automobile” using these two models in Fig. 5c to take a deeper look. Concretely, we use a Chinese phrase list from Jieba³ as the candidate list, which contains 347,728 phrases. Then we obtain the text embeddings of all candidates using RoBERTa-large and BriVL w/ RoBERTa-large, respectively. For each model and each category name, we compute the category name embedding and retrieve top-30 phrases by comparing it with all candidate embeddings using the cosine similarity. Finally, we visualize the results with the UMAP algorithm [42]. For “sports”, we can see that our BriVL relates it to phrases with a higher variety than RoBERTa-large does. However, for “automobile”, the retrieved top-30 phrases of our BriVL are more monotonous.

Cross-Modal Retrieval. Since our BriVL is pre-trained with Chinese data, we choose the only available multimodal Chinese dataset AIC-ICC [43] for performance evaluation in the cross-modal retrieval downstream task. AIC-ICC is originally designed for image captioning, which was first released in AI Challenger 2017, a competition organized by Sinovation Ventures, Sogou, and Toutiao (ByteDance). The training set of AIC-ICC has 300K images and the validation set has 30K images. Each image has 5 Chinese captions. Since the test set is not released, we take the first 10K images along with their corresponding 50K pieces of texts from the validation set for testing.

The cross-modal retrieval results on AIC-ICC are shown in the table of Fig. 6a. The method “BriVL (direct training)” means that we directly train a randomly-initialized BriVL model on the training set of AIC-ICC rather than using the pre-trained BriVL. Moreover, the results of three “BriVL (pre-train & finetune)” variations are all obtained by finetuning the pre-trained BriVL on the training set of AIC-ICC with different finetuning strategies. We only consider two finetuning factors: whether to fix all the batch normalization (BN) layers in the CNN (i.e.,

³<https://github.com/fxsjy/jieba>


a

Method	Fix BN	# Unfixed Blocks	Image-to-Text Retrieval			Text-to-Image Retrieval			
			Recall@1	Recall@5	Recall@10	Recall@1	Recall@5	Recall@10	Recall@SUM
BriVL (direct training)	no	4	36.03	59.48	69.71	28.66	54.33	65.26	317.47
BriVL (pre-train & finetune)	no	2	43.05	65.11	74.57	32.49	57.53	67.99	342.74
BriVL (pre-train & finetune)	no	4	44.49	67.14	75.63	33.67	58.76	68.80	352.49
BriVL (pre-train & finetune)	yes	4	45.61	68.01	76.31	34.06	58.86	69.09	355.94


b

Method	Fix BN	# Unfixed Blocks	Question Type						Overall
			What	Where	When	Who	Why	How	
BriVL (direct training)	no	4	70.51	71.99	81.88	77.05	78.36	68.62	72.16
BriVL (pre-train & finetune)	no	2	79.89	81.71	87.78	84.48	82.66	76.31	80.67
BriVL (pre-train & finetune)	no	4	79.41	81.66	87.31	84.46	83.11	74.44	80.16
BriVL (pre-train & finetune)	yes	4	77.79	80.50	87.99	84.44	82.46	72.87	78.96


c




Why is the train blurry?
A. Moving fast.
B. Bad weather.
C. It's raining.
D. It's nighttime.
BriVL (direct training): C
BriVL (pre-train & finetune): A



How many people are playing?
A. Two.
B. Three.
C. Four.
D. Five.
BriVL (direct training): A
BriVL (pre-train & finetune): B



What are the boats doing?
A. Floating.
B. Sailing.
C. Getting cleaned.
D. Not moving.
BriVL (direct training): A
BriVL (pre-train & finetune): D



Why is the traffic stopped?
A. Car accident.
B. Traffic.
C. Red light.
D. Parade.
BriVL (direct training): B
BriVL (pre-train & finetune): C

Fig. 6: **Cross-modal retrieval and visual question answering results.** **a.** Cross-modal retrieval results (%) on the Chinese dataset AIC-ICC. **b.** Visual question answering results on Visual7W. Overall accuracies (%) along with results on each question type are reported. The dataset is translated into Chinese. **c.** Visual question answering examples of our BriVL model regarding whether it is pre-trained.

EfficientNet-B7), and how many blocks should be unfixed in the CNN. We perform both image-to-text and text-to-image retrieval for evaluation, and report the results with Recall@ k ($k = 1, 5, 10$) as well as Recall@SUM (i.e., the summation of six Recall@ k metrics).

We can observe from the table of Fig. 6a that image-to-text retrieval results are generally higher than text-to-image ones, which is expected because like us humans, describing a given image is easier than imagining a picture from a sentence. We can also see that “BriVL (pre-train & finetune)” variations achieve far better results than “BriVL (direct training)” for all evaluation metrics, indicating the usefulness of large-scale multimodal pre-training. In addition, using pre-trained models like our BriVL is more beneficial to image-to-text retrieval than to text-to-image retrieval, which may be due to the fact that image-to-text retrieval is an easier task. From the performance of three “BriVL (pre-train & finetune)” variations, we find that different finetuning strategies do affect the final results, which should be kept in mind when we finetune pre-trained models for different downstream tasks.

Visual Question Answering. We consider another multimodal task called visual question answering (VQA) [44] on the Visual7W dataset [45]. Visual7W has 47.3K images from MSCOCO [46] and each image comes with a question and four answer candidates, where only one is the correct answer. The whole dataset can be divided into “Telling” questions and “Pointing” ones. Since “Pointing” questions rely on the bounding boxes of objects in images, we only conduct experiments on the “Telling” part, which can be further divided into six question types: “What”, “Where”, “When”, “Who”, “Why”, and “How”. We randomly make the training and test splits with 70% and 30%, respectively. Since Visual7W is an English dataset, we translate all of the questions and answer candidates into Chinese.

In the table of Fig. 6b, we report the overall accuracies on the test set, as well as the results on each question type. Similar to the situation on the cross-modal retrieval task, three “BriVL (pre-train & finetune)” variations achieve much better results than “BriVL (direct training)” for all question types, again indicating the usefulness of large-scale pre-training on downstream tasks. We also notice that the best finetuning strategy for cross-modal retrieval (i.e., fixing BN and keeping 4 blocks of the CNN unfixed) is no longer the best for VQA. In addition, although the strategy of

not fixing BN and keeping 2 blocks unfixed obtains the best overall result, it does not achieve the best for all question types. This is expected as different tasks require different finetuning strategies.

Furthermore, we present four VQA examples in Fig. 6c. From these examples, we see our pre-trained BriVL showing hints of common sense as it knows that the train in the picture looks blurry because it is moving fast, the boats being tied to the dock are simply not moving instead of floating, and the traffic is stopped because of the red light instead of traffic jam. We believe that this is achieved by pre-training with our weak semantic correlation data: the texts are not detailed descriptions of their corresponding images, and thus our BriVL has to figure out the complicated connections hidden among this weak correlation data during pre-training. With extremely large pre-training data as much as 650 million, our BriVL finally succeeds in learning some common sense.

Discussion

We have developed a large-scale multimodal foundation model called BriVL, which is efficiently trained on weak semantic correlation dataset (WSCD) consisting of 650 million image-text pairs. We identified the direct evidence of the aligned image-text embedding space by neural network visualizations, and also demonstrated the cross-modal understanding ability of our BriVL by text-to-image generation. For the first time, we have visually revealed how a multimodal foundation model understands language (e.g., words and sentences). Moreover, extensive experiments on other downstream tasks show the cross-domain learning/transfer ability of our BriVL and the advantage of multimodal learning over single-modal learning. Particularly, our BriVL appears to acquire abilities in reasoning and imagination. Last but not least, we believe that all of these advantages are mainly due to the weak semantic correlation assumption followed by our BriVL. That is, by effectively fusing the complex human emotions and thoughts from those weakly correlated image-text pairs, our BriVL is made more cognitive and general (i.e., much closer to AGI).

We believe that the solid step we take towards AGI would have a broad impact not only on the AI development community but also on a wide range of AI+ fields. For the AI research field itself, based on our GPU-resource-saving multimodal pre-training framework, researchers could easily extend our BriVL to a larger capacity with more modalities, leading to more general foundation models. Moreover, with the help of large-scale multimodal foundation models, it would also be much easier for researchers to explore novel tasks (especially those without abundant human-annotated samples). For AI+ fields, such foundation models could be quickly adapted to specific working context or environment, thanks to their strong generalization abilities. For example, in healthcare, multimodal foundation models could make full use of case data in multi-modality (e.g., computed tomography data, and blood routine examination data) to improve the diagnosing accuracy. Moreover, in neuroscience, multimodal foundation models could even help find out the mechanism of how multimodal data connect and fuse since artificial neural networks are much simpler to examine than real neural systems in human brains.

Nevertheless, multimodal foundation models still face potential risks and challenges. Since the performance of foundation models is based on the data that they are pre-trained on, it is likely that the models learn prejudices and stereotypes about certain issues, which should be carefully handled before model training and monitored/addressed in downstream applications. Moreover, as foundation models master more and more skills, creators of these models should be aware of model misuse by ill-intentioned people (e.g., manipulating or generating fake contents), which would have a negative influence on the society. In addition, on the evolution challenges of foundation models academically, it is of grand challenge for (1) developing model-interpretability tools deeper into the foundation models, (2) constructing huge pre-training datasets with more modalities, as well as (3) applying foundation models to various downstream tasks with more effective adaptation/finetuning techniques.

Our understanding of what BriVL (or any large-scale multimodal foundation model) has learned and what it is capable of has only just started. There is still much room for further study to better understand the foundation model and develop more novel use cases. For instance, since image can be regarded as a universally-understood “language”, soliciting an even larger dataset containing multiple languages could result in a language translation model obtained as a by-product of multimodal pre-training. Moreover, additional modalities (e.g., videos and audios) can be also explored to pre-train a more intelligent model, taking us even closer to AGI.

Methods

Architecture Overview. The notion of pre-training a large-scale machine learning model and then using it for downstream tasks first appeared in natural language processing (NLP). As shown in Supplementary Note Fig. S1c, large-scale NLP models like GPT [47], BERT [48], and their variants, take Transformers [49] as text encoders to encode input texts into text embeddings, and then design pre-training objectives on top of these embeddings (e.g., generative loss and masked language modeling loss). In computer vision (CV), large-scale pre-training also becomes popular.

Models like BiT [50] and ViT [51] use convolutional neural networks (CNNs) or Transformers as image encoders to obtain embeddings of input images. Similarly, pre-training losses are computed using the image embeddings (e.g., image classification loss and masked image patch prediction loss). However, these models are single-modal and thus only benefit downstream tasks in one modality. For multimodal (e.g., image, text, and audio) pre-training [11–17, 31], existing works can be divided into two groups according to their network architectures: single-tower models (e.g., UNITER [16], OSCAR [11], and M6 [17]) and two-tower ones (e.g., CLIP [12] and ALIGN [31]). Our BriVL can also be categorized into the two-tower models since we use separate image and text encoders. But note that we actually adopt two additional momentum encoders to help with the pre-training process (i.e., to dynamically maintain negative sample queues across training batches), resulting in a four-tower pre-training architecture.

The pre-training goal of our BriVL is to learn two encoders that can embed image and text inputs into the same semantic space for effective image-text retrieval. To enforce the image and text encoders to learn better representations in the same embedding space, we introduce cross-modal contrastive learning with the InfoNCE loss [22] into our BriVL. Specifically, our learning objective is to find the corresponding image embedding from a batch of them for a given text embedding and vice versa. By maximizing the cosine similarity of the image and text embeddings for each ground-truth pair while minimizing the cosine similarities of the embeddings from negative pairs, we jointly train the image and text encoders to learn an aligned cross-modal embedding space.

Formally, for the image-text retrieval task, we denote the training set as $\mathcal{D} = \{(x_i^{(i)}, x_i^{(t)}) | i = 1, \dots, N\}$, where $(x_i^{(i)}, x_i^{(t)})$ is a matched image-text pair, and N is the size of \mathcal{D} . Our BriVL leverages contrastive learning by applying MoCo [28] into the cross-modal scenario, as illustrated in Supplementary Note Fig. S1a. Each image $x_i^{(i)}$ (or each text $x_i^{(t)}$) is encoded by the image encoder $f^{(i)}$ (or the text encoder $f^{(t)}$) to obtain its d -dimensional embedding $\mathbf{z}_i^{(i)}$ (or $\mathbf{z}_i^{(t)}$). The image encoder (see Supplementary Note Fig. S1b) contains a CNN backbone, a successive self-attention (SA) block, and a multi-layer perceptron (MLP). A sequence of patch embeddings are first obtained by applying multi-scale patch pooling (MSPP) to the feature map from CNN. They are then fused/encoded by the SA block. The text encoder, on the other hand, is stacked by several SA blocks such as BERT [48] and RoBERTa [4]. A two-layer MLP block with a ReLU [52] activation layer is used for mapping each encoder’s representation into the joint cross-modal embedding space. The parameters of $f^{(i)}$ and $f^{(t)}$ are denoted as $\theta^{(i)}$ and $\theta^{(t)}$, respectively.

Image Encoder. To obtain better performance in the image-text retrieval task, most previous methods [18–20, 53] utilize a bottom-up attention mechanism [54] with object features extracted by the Faster R-CNN detector [55]. However, extracting region/object features with a heavy detector is computationally expensive, e.g., a Faster R-CNN detector typically costs 0.064s (15.6fps) to extract fine-grained region information from an image of moderate size. Meanwhile, the image-text retrieval would be inevitably limited by the detector’s performance, which is not adaptable to real-world applications. In this paper, we thus introduce a simple yet effective module named Multi-Scale Patch Pooling (MSPP) to address this problem.

For each input image $x^{(i)}$, we first split it into multiple patches at different scales and record the patch coordinates. In all experiments, we take two scales as 1×1 and 6×6 , resulting in a total of 37 patches. Next, we project each set of patch coordinates onto the feature map that is obtained by the CNN backbone (e.g., EfficientNet [41]) and generate a sequence of 37 region feature maps. Finally, we apply average pooling to each region feature map and obtain a sequence of patch features $\mathbf{S} \in \mathbb{R}^{c \times N_p}$, where each column corresponds to a patch, N_p is the number of patches (i.e., $N_p = 37$ in this paper), and c is the number of channels in the feature map.

To better capture the relationship of image patch features, we deploy a self-attention (SA) block containing multiple Transformer [49] encoder layers. Each Transformer encoder layer consists of a multi-head attention (MultiHeadAttn) layer and a feed forward network (FFN) layer:

$$\mathbf{S}' = \text{LayerNorm}(\mathbf{S} + \text{MultiHeadAttn}(\mathbf{S})), \quad (1)$$

$$\mathbf{S} = \text{LayerNorm}(\mathbf{S}' + \text{FFN}(\mathbf{S}')). \quad (2)$$

We then fuse the extracted patch features by applying an average pooling layer:

$$\mathbf{r}^{(i)} = \frac{1}{N_p} \sum_{j=1}^{N_p} \mathbf{S}_j \in \mathbb{R}^c, \quad (3)$$

where \mathbf{S}_j is the j -th column of \mathbf{S} . A two-layer MLP block with a ReLU activation layer is adopted to project $\mathbf{r}^{(i)}$ to the joint cross-modal embedding space, resulting in the final d -dimensional image embedding $\mathbf{z}^{(i)} \in \mathbb{R}^d$.

Text Encoder. Given a sentence $x^{(t)}$, we first tokenize it to obtain a sequence of tokens $\mathcal{T} = \{\mathbf{t}_j | j = 1, \dots, l\}$, where l denotes the length of the sentence (e.g., the number of words) and \mathbf{t}_j denotes the j -th token of \mathcal{T} . A pre-trained

Transformer encoder (e.g., RoBERTa [40]) is then used to map text tokens to a sequence of feature vectors (each feature vector corresponds to a word). Similarly, to better capture the relationship between words, we use the same self-attention mechanism as in the image encoder to extract the text representation $\mathbf{r}^{(t)}$. A two-layer MLP block with a ReLU activation layer is also used for mapping the text representation $\mathbf{r}^{(t)}$ to the joint cross-modal embedding space, resulting in the final d -dimensional text embedding $\mathbf{z}^{(t)} \in \mathbb{R}^d$.

Contrastive Loss. The cross-modal contrastive loss in our BriVL is defined based on MoCo [28], which provides a mechanism of building dynamic sample queues for contrastive learning. Since the two negative queues used in our BriVL decouple the queue size from the mini-batch size, we can have a much larger negative sample size than the mini-batch size (thus GPU-resource-saving).

To maintain large queues of samples coming from different mini-batches and address the problem that sample features are extracted by encoders with very different parameters, we need two more smoothly updated encoders, that is, momentum encoders. The parameters $\theta_m^{(i)}$ (or $\theta_m^{(t)}$) of the momentum image encoder $f_m^{(i)}$ (or the momentum text encoder $f_m^{(t)}$) are updated in each training iteration with a momentum hyper-parameter m :

$$\theta_m^{(i)} = m \cdot \theta_m^{(i)} + (1 - m) \cdot \theta^{(i)}, \quad (4)$$

$$\theta_m^{(t)} = m \cdot \theta_m^{(t)} + (1 - m) \cdot \theta^{(t)}. \quad (5)$$

Further, we maintain two negative sample queues $\mathcal{Q}^{(i)}$ and $\mathcal{Q}^{(t)}$, which contain N_q image negatives and N_q text negatives for contrastive learning, respectively. In each pre-training iteration with the batch size N_b , all N_b image negatives and N_b text negatives are separately pushed into these two queues. Meanwhile, there are N_b earliest samples being popped out of each queue. Concretely, at iteration t , the image and text negatives from the current data batch ($\mathcal{B}_t^{(i)}, \mathcal{B}_t^{(t)}$) are computed by respectively forwarding the momentum encoders $f_m^{(i)}$ and $f_m^{(t)}$:

$$\mathcal{N}_t^{(i)} = \{f_m^{(i)}(x_i^{(i)}) | x_i^{(i)} \in \mathcal{B}_t^{(i)}\}, \quad (6)$$

$$\mathcal{N}_t^{(t)} = \{f_m^{(t)}(x_i^{(t)}) | x_i^{(t)} \in \mathcal{B}_t^{(t)}\}, \quad (7)$$

where $|\mathcal{B}_t^{(i)}| = |\mathcal{B}_t^{(t)}| = N_b$. The obtained $\mathcal{N}_t^{(i)}$ and $\mathcal{N}_t^{(t)}$ are then pushed into $\mathcal{Q}^{(i)}$ and $\mathcal{Q}^{(t)}$, respectively. Note that although we generally call $\mathcal{N}_t^{(i)}$ (or $\mathcal{N}_t^{(t)}$) image negatives (or text negatives), there is still one sample being positive to each text (or image). Here, we denote the positive image sample (or text sample) for the j -th input text $x_j^{(t)}$ (or the j -th input image $x_j^{(i)}$) of the current mini-batch as:

$$\mathbf{p}_j^{(i)} = f_m^{(i)}(x_j^{(i)}) \in \mathcal{N}_t^{(i)}, \quad (8)$$

$$\mathbf{p}_j^{(t)} = f_m^{(t)}(x_j^{(t)}) \in \mathcal{N}_t^{(t)}. \quad (9)$$

With the two negative queues, the loss function in each training iteration is thus computed as follows. For each input image $x_i^{(i)}$, we define the contrastive loss between its image embedding $\mathbf{z}_i^{(i)}$ and all positive/negative texts in the queue $\mathcal{Q}^{(t)}$ as an InfoNCE loss [22]:

$$\mathcal{L}_{i2t} = -\frac{1}{N_b} \sum_i \log \frac{\exp(\mathbf{z}_i^{(i)} \cdot \mathbf{p}_i^{(t)} / \tau)}{\exp(\mathbf{z}_i^{(i)} \cdot \mathbf{p}_i^{(t)} / \tau) + \sum_{\mathbf{n}^{(t)}} \exp(\mathbf{z}_i^{(i)} \cdot \mathbf{n}^{(t)} / \tau)}, \quad (10)$$

where $\mathbf{n}^{(t)} \in \mathcal{Q}^{(t)} \setminus \{\mathbf{p}_i^{(t)}\}$ denotes a text negative for each image, τ is the temperature hyper-parameter, and the vector similarity is measured by dot product (\cdot). Similarly, for each input text $x_i^{(t)}$, the InfoNCE loss is given by:

$$\mathcal{L}_{t2i} = -\frac{1}{N_b} \sum_i \log \frac{\exp(\mathbf{z}_i^{(t)} \cdot \mathbf{p}_i^{(i)} / \tau)}{\exp(\mathbf{z}_i^{(t)} \cdot \mathbf{p}_i^{(i)} / \tau) + \sum_{\mathbf{n}^{(i)}} \exp(\mathbf{z}_i^{(t)} \cdot \mathbf{n}^{(i)} / \tau)}, \quad (11)$$

where $\mathbf{n}^{(i)} \in \mathcal{Q}^{(i)} \setminus \{\mathbf{p}_i^{(i)}\}$ denotes an image negative for each text.

The total loss function for pre-training our BriVL is then defined as:

$$\mathcal{L}_{total} = \mathcal{L}_{i2t} + \mathcal{L}_{t2i}. \quad (12)$$

In the test/evaluation stage, given each query image (or text), the cross-modal retrieval results are obtained simply by the dot product defined over the outputs of the text (or image) encoder.

Implementation Details. Over the input images, we adopt random graying and random color jittering for data augmentation. All images are resized to 600×600 pixels. We adopt EfficientNet-B7 [41] as the CNN backbone in the image encoder and RoBERTa-Large [40] as the basis Transformer in the text encoder. For both image and text encoders, the self-attention block consists of 4 Transformer encoder layers and the MLP block has two fully-connected layers with a ReLU activation layer. The final embedding size of the joint cross-modal space is 2,560. We select the hyper-parameters heuristically for pre-training our BriVL model due to the computational constraint: the temperature hyper-parameter $\tau = 0.07$, momentum $m = 0.99$, and the queue size $N_q = 13,440$. We adopt the Adam optimizer [56], with the weight decay $1e-5$ and the learning rate $1e-4$. We use a mini-batch size of 192 for each of the 14 machines (each machine has 8 NVIDIA A100 GPUs), resulting in a total batch size of 2,688 (far smaller than N_q). The resource-saving advantages of such batch setting are shown by the ablation study results in Supplementary Note Fig. S2. We also deploy the latest distributed-training framework DeepSpeed [25] to accelerate the pre-training process and save the GPU memories. With 112 NVIDIA A100 GPUs in total, it takes about 10 days to pre-train our BriVL model over our WSCD of 650 million image-text pairs.

Differences from CLIP/ALIGN. We have stated two main differences between our BriVL and CLIP/ALIGN in the Main section. Below we give more detailed differences technically. (1) We adopt a four-tower network architecture (see Supplementary Note Fig. S1a) for pre-training. By extending the original single-modal contrastive learning (CL) algorithm MoCo [28], we introduce momentum encoders and negative sample queues for multimodal pre-training in a more GPU-resource-saving way. In contrast, both CLIP and ALIGN employ the standard two-tower architecture, which requires large batch size (thus enough negative samples) to be effective, taking up a mass of GPU memories. (2) We additionally devise a multi-scale patch pooling (MSPP) module (see Supplementary Note Fig. S1b) to capture fine-grained image region representations without using object detectors. While CLIP and ALIGN only consider global-level image embeddings, which impedes their ability to learn fine-grained/local image features.

Acknowledgments

This work was supported in part by National Natural Science Foundation of China (61976220 and 61832017), Beijing Outstanding Young Scientist Program (BJJWZYJH012019100020098), and Large-Scale Pre-Training Program of Beijing Academy of Artificial Intelligence (BAAI).

Corresponding Authors

Correspondence to Zhiwu Lu (luzhiwu@ruc.edu.cn), Hao Sun (haosun@ruc.edu.cn) or Ji-Rong Wen (jrwen@ruc.edu.cn).

References

- [1] Goertzel, B. Artificial general intelligence: Concept, state of the art, and future prospects. *Journal of Artificial General Intelligence* **5**, 1–48 (2014).
- [2] LeCun, Y., Bengio, Y. & Hinton, G. Deep learning. *Nature* **521**, 436–444 (2015).
- [3] He, K., Zhang, X., Ren, S. & Sun, J. Deep residual learning for image recognition. In *IEEE Conference on Computer Vision and Pattern Recognition*, 770–778 (2016).
- [4] Liu, Y. *et al.* Roberta: A robustly optimized bert pretraining approach. *arXiv preprint arXiv:1907.11692* (2019).
- [5] Wang, A. *et al.* GLUE: A multi-task benchmark and analysis platform for natural language understanding. In *International Conference on Learning Representations* (2019).
- [6] Santoro, A. *et al.* A simple neural network module for relational reasoning. In *Advances in Neural Information Processing Systems*, 4967–4976 (2017).
- [7] Bommasani, R. *et al.* On the opportunities and risks of foundation models. *arXiv preprint arXiv:2108.07258* (2021).
- [8] Brown, T. B. *et al.* Language models are few-shot learners. In *Advances in Neural Information Processing Systems*, 1877–1901 (2020).

- [9] Quiroga, R. Q., Reddy, L., Kreiman, G., Koch, C. & Fried, I. Invariant visual representation by single neurons in the human brain. *Nature* **435**, 1102–1107 (2005).
- [10] Quian Quiroga, R., Kraskov, A., Koch, C. & Fried, I. Explicit encoding of multimodal percepts by single neurons in the human brain. *Current Biology* **19**, 1308–1313 (2009).
- [11] Li, X. *et al.* Oscar: Object-semantics aligned pre-training for vision-language tasks. In *European Conference on Computer Vision*, 121–137 (2020).
- [12] Radford, A. *et al.* Learning transferable visual models from natural language supervision. In *International Conference on Machine Learning*, 8748–8763 (2021).
- [13] Li, L. H., Yatskar, M., Yin, D., Hsieh, C. & Chang, K. Visualbert: A simple and performant baseline for vision and language. *arXiv preprint arXiv:1908.03557* (2019).
- [14] Li, G., Duan, N., Fang, Y., Gong, M. & Jiang, D. Unicoder-vl: A universal encoder for vision and language by cross-modal pre-training. In *AAAI Conference on Artificial Intelligence*, 11336–11344 (2020).
- [15] Su, W. *et al.* VL-BERT: pre-training of generic visual-linguistic representations. In *International Conference on Learning Representations* (2020).
- [16] Chen, Y.-C. *et al.* Uniter: Universal image-text representation learning. In *European Conference on Computer Vision*, 104–120 (2020).
- [17] Lin, J. *et al.* M6: A chinese multimodal pretrainer. *arXiv preprint arXiv:2103.00823* (2021).
- [18] Wu, Y., Wang, S., Song, G. & Huang, Q. Learning fragment self-attention embeddings for image-text matching. In *ACM International Conference on Multimedia*, 2088–2096 (2019).
- [19] Chen, H. *et al.* Imram: Iterative matching with recurrent attention memory for cross-modal image-text retrieval. In *IEEE Conference on Computer Vision and Pattern Recognition*, 12655–12663 (2020).
- [20] Diao, H., Zhang, Y., Ma, L. & Lu, H. Similarity reasoning and filtration for image-text matching. In *AAAI Conference on Artificial Intelligence*, 1218–1226 (2021).
- [21] Wu, Z., Xiong, Y., Yu, S. X. & Lin, D. Unsupervised feature learning via non-parametric instance discrimination. In *IEEE Conference on Computer Vision and Pattern Recognition*, 3733–3742 (2018).
- [22] Oord, A. v. d., Li, Y. & Vinyals, O. Representation learning with contrastive predictive coding. *arXiv preprint arXiv:1807.03748* (2018).
- [23] Hjelm, R. D. *et al.* Learning deep representations by mutual information estimation and maximization. In *International Conference on Learning Representations* (2019).
- [24] Zhuang, C., Zhai, A. L. & Yamins, D. Local aggregation for unsupervised learning of visual embeddings. In *International Conference on Computer Vision*, 6002–6012 (2019).
- [25] Rajbhandari, S., Ruwase, O., Rasley, J., Smith, S. & He, Y. Zero-infinity: Breaking the GPU memory wall for extreme scale deep learning. *arXiv preprint arXiv:2104.07857* (2021).
- [26] Riquelme, C. *et al.* Scaling vision with sparse mixture of experts. *arXiv preprint arXiv:2106.05974* (2021).
- [27] Chen, T., Kornblith, S., Norouzi, M. & Hinton, G. A simple framework for contrastive learning of visual representations. In *International Conference on Machine Learning*, 1597–1607 (2020).
- [28] He, K., Fan, H., Wu, Y., Xie, S. & Girshick, R. Momentum contrast for unsupervised visual representation learning. In *IEEE Conference on Computer Vision and Pattern Recognition*, 9729–9738 (2020).
- [29] Grill, J.-B. *et al.* Bootstrap your own latent - a new approach to self-supervised learning. In *Advances in Neural Information Processing Systems*, 21271–21284 (2020).
- [30] Chen, X. & He, K. Exploring simple siamese representation learning. In *IEEE Conference on Computer Vision and Pattern Recognition*, 15750–15758 (2021).
- [31] Jia, C. *et al.* Scaling up visual and vision-language representation learning with noisy text supervision. In *International Conference on Machine Learning*, 4904–4916 (2021).

- [32] Olah, C., Mordvintsev, A. & Schubert, L. Feature visualization. *Distill* (2017).
- [33] Esser, P., Rombach, R. & Ommer, B. Taming transformers for high-resolution image synthesis. *arXiv preprint arXiv:2012.09841* (2020).
- [34] Russakovsky, O. *et al.* Imagenet large scale visual recognition challenge. *International Journal of Computer Vision* **115**, 211–252 (2015).
- [35] Yang, Y. & Newsam, S. D. Bag-of-visual-words and spatial extensions for land-use classification. In *International Symposium on Advances in Geographic Information Systems*, 270–279 (2010).
- [36] Xia, G.-S. *et al.* Aid: A benchmark data set for performance evaluation of aerial scene classification. *IEEE Transactions on Geoscience and Remote Sensing* **55**, 3965–3981 (2017).
- [37] Guan, J. *et al.* Zero and few shot learning with semantic feature synthesis and competitive learning. *IEEE Transactions on Pattern Analysis and Machine Intelligence* **43**, 2510–2523 (2021).
- [38] Li, A., Lu, Z., Wang, L., Xiang, T. & Wen, J. Zero-shot scene classification for high spatial resolution remote sensing images. *IEEE Transactions on Geoscience and Remote Sensing* **55**, 4157–4167 (2017).
- [39] Li, J., Sun, M. & Zhang, X. A comparison and semi-quantitative analysis of words and character-bigrams as features in chinese text categorization. In *Proc. 21st International Conference on Computational Linguistics and 44th Annual Meeting of the Association for Computational Linguistics*, 545–552 (2006).
- [40] Cui, Y. *et al.* Revisiting pre-trained models for chinese natural language processing. In *Conference on Empirical Methods in Natural Language Processing: Findings*, 657–668 (2020).
- [41] Tan, M. & Le, Q. Efficientnet: Rethinking model scaling for convolutional neural networks. In *International Conference on Machine Learning*, 6105–6114 (2019).
- [42] McInnes, L., Healy, J., Saul, N. & Großberger, L. UMAP: uniform manifold approximation and projection. *Journal of Open Source Software* **3**, 861 (2018).
- [43] Wu, J. *et al.* Ai challenger: A large-scale dataset for going deeper in image understanding. *arXiv preprint arXiv:1711.06475* (2017).
- [44] Niu, Y. *et al.* Counterfactual VQA: A cause-effect look at language bias. In *IEEE Conference on Computer Vision and Pattern Recognition*, 12700–12710 (2021).
- [45] Zhu, Y., Groth, O., Bernstein, M. S. & Fei-Fei, L. Visual7w: Grounded question answering in images. In *IEEE Conference on Computer Vision and Pattern Recognition*, 4995–5004 (2016).
- [46] Lin, T.-Y. *et al.* Microsoft coco: Common objects in context. In *European Conference on Computer Vision*, 740–755 (2014).
- [47] Radford, A., Narasimhan, K., Salimans, T. & Sutskever, I. Improving language understanding by generative pre-training. *OpenAI Blog* (2018).
- [48] Devlin, J., Chang, M.-W., Lee, K. & Toutanova, K. Bert: Pre-training of deep bidirectional transformers for language understanding. *arXiv preprint arXiv:1810.04805* (2018).
- [49] Vaswani, A. *et al.* Attention is all you need. In *Advances in Neural Information Processing Systems*, 5998–6008 (2017).
- [50] Kolesnikov, A. *et al.* Big transfer (bit): General visual representation learning. In *European Conference on Computer Vision*, 491–507 (2020).
- [51] Dosovitskiy, A. *et al.* An image is worth 16x16 words: Transformers for image recognition at scale. In *International Conference on Learning Representations* (2021).
- [52] Nair, V. & Hinton, G. E. Rectified linear units improve restricted boltzmann machines. In *International Conference on Machine Learning*, 807–814 (2010).
- [53] Wei, X., Zhang, T., Li, Y., Zhang, Y. & Wu, F. Multi-modality cross attention network for image and sentence matching. In *IEEE Conference on Computer Vision and Pattern Recognition*, 10941–10950 (2020).

- [54] Anderson, P. *et al.* Bottom-up and top-down attention for image captioning and visual question answering. In *IEEE Conference on Computer Vision and Pattern Recognition*, 6077–6086 (2018).
- [55] Ren, S., He, K., Girshick, R. B. & Sun, J. Faster R-CNN: towards real-time object detection with region proposal networks. In *Advances in Neural Information Processing Systems*, 91–99 (2015).
- [56] Kingma, D. P. & Ba, J. Adam: A method for stochastic optimization. In *International Conference on Learning Representations* (2015).
- [57] Young, P., Lai, A., Hodosh, M. & Hockenmaier, J. From image descriptions to visual denotations: New similarity metrics for semantic inference over event descriptions. *Transactions of the Association for Computational Linguistics* **2**, 67–78 (2014).
- [58] Ordonez, V., Kulkarni, G. & Berg, T. L. Im2text: Describing images using 1 million captioned photographs. In *Advances in Neural Information Processing Systems*, 1143–1151 (2011).
- [59] Sharma, P., Ding, N., Goodman, S. & Soricut, R. Conceptual captions: A cleaned, hypernymed, image alt-text dataset for automatic image captioning. In *Proceedings of the 56th Annual Meeting of the Association for Computational Linguistics*, 2556–2565 (2018).

– Supplementary Note –

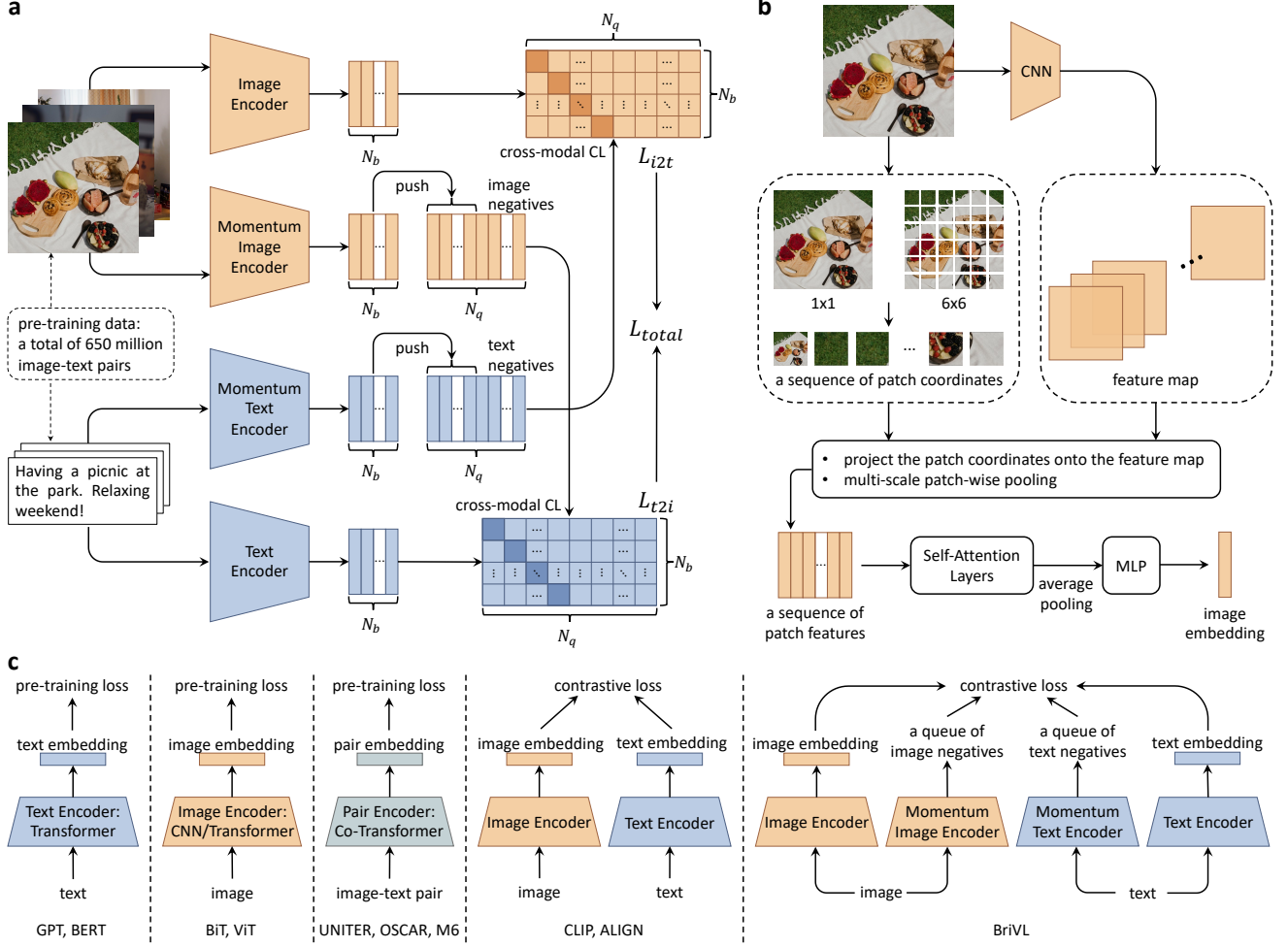


Fig. S1: **Illustrations of our algorithm design, our network design, and existing pre-training architectures.** **a.** The schematic illustration of the proposed BriVL model for large-scale multimodal pre-training. **b.** The detailed network architecture of our image encoder in BriVL. **c.** Illustration of existing pre-training architectures. From left to right: single-modal textual pre-training (e.g., GPT [47] and BERT [48]); single-modal visual pre-training (e.g., BiT [50] and ViT [51]); single-tower multimodal pre-training (e.g., UNITER [16], OSCAR [11], and M6 [17]); two-tower multimodal pre-training (e.g., CLIP [12] and ALIGN [31]); our BriVL.

Architecture Overview

In Fig. S1a, we present the schematic illustration of our proposed BriVL model for large-scale multimodal pre-training. In Fig. S1b, we show the network details of our image encoder in BriVL. In Fig. S1c, existing architectures for pre-training are illustrated. Please see Methods of the main manuscript for more information.

Ablation Study

To show the contributions of the self-attention (SA) layers used in both encoders and the cross-modal contrastive loss based on MoCo [28], we conduct experiments by whether using SA layers and adopting alternative contrastive losses. Since it is too costly to conduct the ablation study on our full WSCD dataset (of 650M image-text pairs), we only use 22M image-text pairs for training and another 11K for evaluation. We provide the same 9 machines (each has 8 NVIDIA A100 GPUs) for all ablation experiments. The compared methods are as follows: (1) BriVL w/ BYOL: We replace the MoCo-based cross-modal contrastive algorithm in our standard BriVL model with BYOL [29], which does not need any negative samples and only focuses on matching the positive ones. (2) BriVL w/ SimCLR: We replace the MoCo-based cross-modal contrastive algorithm with SimCLR [27], which does not have momentum

a

Method	w/ SA Layers?	Contrastive Algorithm	Image-to-Text Retrieval			Text-to-Image Retrieval			
			Recall@1	Recall@5	Recall@10	Recall@1	Recall@5	Recall@10	Recall@SUM
BriVL w/ SimCLR	yes	SimCLR-based	27.50	47.32	55.50	27.10	46.84	55.19	259.45
BriVL w/o SA	no	MoCo-based	28.56	47.98	55.83	28.02	46.86	54.58	261.83
BriVL	yes	MoCo-based	29.82	49.13	56.47	29.28	48.12	55.84	268.66

b













Query	Retrieval Results				
	Top1	Top2	Top3	Top4	Top5
	Drinking tea often when there is nothing wrong with it can help you to cultivate your body and improve your sex, and it can also reduce the body's cholesterol and triglyceride content.	Cherish your busy time, being busy is the most precious medicine in the world. Busy people are happy, because there is something to do, life is valuable.	People are like grass and mustards, life is easy to break, and cherish life is precious, not wasteful.	Keeping an optimistic life is the mood, and people live the mentality. Life is precious. Instead of worrying too much about complicated and trivial matters, it is better to treat yourself and relax your life.	"Know yourself and the enemy, a hundred battles will never be lost." This is the truth drawn from practice. No matter what kind of industry you are in, the important prerequisite for success is to "know yourself".
	Recently, after Megan Harry announced her withdrawal from the royal family, Kate also took over all major events. He was very diligent in frequent public appearances. In terms of styling, it is still the same.	In the play, the "H" version of the design was restored, and the queen's iconic three-quarter sleeves were especially noticed. The Queen of England loves to set the sleeve length of the suit to 70%.	Leonor has a very good relationship with his parents, especially close to his father, because after all, he is the crown prince, and King Felipe will lead her by precept and deeds.	Kate's Dolce&Gabbana green one-piece dress, which is the same as the first time worn in 2016, also shows the body.	Even with the video connection, Princess Kate still dresses herself up dignified and generously. Princess Kate usually wears private clothes and is almost the object of imitation by the whole people.
At 8 o'clock in the morning on January 29, a plane from Singapore landed. The customs inspection site at Jinan Airport opened a "green channel" for the carriers of donated materials. After checking the documents, an unpacking check was carried out.					
On October 30, in Fullerton, California, USA, firefighters work on the fire scene. In recent days, wildfires in California, the United States, have continued to rage, and a large number of residents have been forced to evacuate.					

Fig. S2: **Quantitative and qualitative results on the 11K test set.** a. Ablative results (%) of BriVL with 22M training data. b. Cross-modal retrieval examples of our standard BriVL model trained on the 22M data. Texts are translated into English for representation clarity.


encoders or negative sample queues, and computes the InfoNCE loss [22] within each batch. In other words, the mini-batch size decides the number of negative samples for each positive image-text pair. Note that CLIP [12] and ALIGN [31] both adopt SimCLR-based contrastive loss. (3) BriVL w/o SA: We discard the SA layers from both image and text encoders comparing to our standard BriVL. (4) BriVL: Our standard model with SA layers and MoCo-based cross-modal contrastive algorithm. All methods are trained for 6 epochs.

The ablative results are shown in the table of Fig. S2a. Note that we do not report the results of BriVL w/ BYOL because no matter how we try (e.g., tuning the hyper-parameters and implementing in different ways), the model always collapses. One possible reason is that BYOL only works under single-modal scenarios and it is essential to include negative samples under multimodal scenarios. Moreover, since SimCLR has neither momentum encoders nor negative sample queues, its mini-batch size N_b can be larger than that of standard BriVL with the same computational resources. Concretely, the total batch size is 2,160 for SimCLR and 1,728 for standard BriVL which additionally maintains two negative sample queues with the size of 10,368⁴. However, we can then see from the table that BriVL w/ SimCLR performs worse than our standard BriVL (based on MoCo) for all 7 evaluation metrics. This indicates the importance of large number of negative samples in multimodal pre-training and the advantage of our standard BriVL when large batch size is not feasible. Our model design thus hopefully helps those researchers with limited GPU resources for multimodal pre-training. Besides, comparing to our standard BriVL, discarding the SA layers (i.e., BriVL w/o SA) also leads to performance drop, which validates the effectiveness of this module.

⁴Since momentum encoders and negative sample queues do not produce gradients, they take up little GPU memory.

Method	Question Type						
	What	Where	When	Who	Why	How	Overall
BriVL-en (direct training)	76.74	77.13	78.12	76.21	76.45	77.55	76.91
BriVL-en (pre-train & zero-shot)	52.40	53.24	53.11	53.29	52.34	52.98	52.75
BriVL-en (pre-train & finetune)	81.20	81.69	81.36	80.45	80.64	81.75	81.26

Method	BLEU @4	METEOR	CIDEr	SPICE	ROUGE-L
BriVL-en (direct training)	18.87	14.44	37.06	12.71	44.01
BriVL-en (pre-train & finetune)	20.18	21.90	44.47	15.54	45.85




BriVL-en (direct training):

- A girl in a white and blue uniform is trying to catch a ball.

BriVL-en (pre-train & finetune):

- A young girl in a softball uniform is throwing a ball.




BriVL-en (direct training):

- A man wearing a mask and a hat is smiling.

BriVL-en (pre-train & finetune):

- A man in a chef's hat and apron is preparing food.



BriVL-en (direct training):

- A woman wearing a red scarf and a child wearing a blue headscarf.

BriVL-en (pre-train & finetune):

- A mother and her daughter are dressed in costumes.

Fig. S3: **Results on two English downstream tasks.** **a.** Visual question answering results on Visual7W. Overall accuracies (%) along with results on each question type are reported. **b.** Image captioning results (%) on the test split of Flickr30K. **c.** Image captioning examples of our BriVL-en model regarding whether it is pre-trained.

Furthermore, in Fig. S2b, we present several examples on the 11K test set with our standard BriVL model trained on the 22M data. We can observe that the returned top-5 texts for the query image containing a cup of tea are all philosophical sentences, validating the effectiveness of training BriVL over weak semantic correlation data. For queries in the rest three rows, BriVL also does a great job in finding the matched contents in the other modality (different from the modality of queries).

Results on English Tasks

In this section, we pre-train our model on an English dataset and name it as BriVL-en. Concretely, the pre-training English dataset consists of 4 publicly-available image captioning datasets. (1) **MSCOCO** [46]: We only use the training split of MSCOCO, which contains 113,287 images (each image has 5 text captions). (2) **Flickr30K** [57]: We use the training set of Flickr30K, which contains 29,783 images (each image also has 5 text captions). (3) **SBU Captioned Photo Dataset (SBU)** [58]: We collect SBU by the provided urls and obtain around 867K image-text pairs. We use the whole SBU dataset. (4) **Conceptual Captions (CC)** [59]: We also collect and use the whole CC dataset, which contains around 3M image-text pairs. As a result, the total size of the pre-training English dataset is around 4M.

In the next two subsections, we conduct experiments on two downstream tasks (i.e., visual question answering and image captioning) to show the potential use of our English model BriVL-en. Importantly, the obtained similar results indicate that our model indeed provides a feasible solution closer to AGI beyond specific languages.

Visual Question Answering. We first conduct visual question answering (VQA) experiments on the Visual7W dataset [45] with three BriVL-en variations. The dataset split is the same as that for Chinese VQA experiments in the main paper, but this time we do not need to translate the texts.

In the table of Fig. S3a, we report the overall accuracies on the test set of Visual7W, as well as the results on each question type. We can make the following observations: (1) “BriVL-en (pre-train & zero-shot)” performs much worse than “BriVL-en (direct training)”. This is mainly because the VQA task has a large domain gap to our pre-training task and the data distributions are also totally different. (2) “BriVL-en (pre-train & finetune)” outperforms “BriVL-en (direct training)” by large margins for all evaluation metrics, indicating the effectiveness of the pre-trained model and also the importance of finetuning when the data distribution of the downstream task is different with that of the pre-training data.

Image Captioning. Image captioning aims to generate descriptions for given images. In the table of Fig. S3b, we report the results on the test split of Flickr30K [57] (1K images) w.r.t. five commonly-used evaluation metrics in the field of image captioning. Since an additional Transformer [49] decoder is needed to generate texts, we cannot conduct zero-shot experiments. We can see that “BriVL-en (pre-train & finetune)” outperforms “BriVL-en (direct training)” for all metrics, again validating the effectiveness of pre-training.

Furthermore, we present three image captioning examples in Fig. S3c. For the first image, “BriVL-en (pre-train & finetune)” points out that the young girl is wearing a softball uniform instead of “a white and blue uniform”, and is trying to throw a ball rather than catching it. Actually it is hard to tell whether the girl is throwing or catching the ball only by this picture. But as long as we know a ball is usually caught by the glove in this sport (which is commonsensical), it is easy to conclude that the girl is throwing the ball. For the second image, “BriVL-en (pre-train & finetune)” knows that the man is a chef wearing an apron instead of a mask, and is preparing food. Here, our pre-trained BriVL-en judges that the man is a chef also by common sense (by his dressing). For the third image, “BriVL-en (pre-train & finetune)” makes a good guess that there are a mother and her daughter in the image instead of just saying a woman and a child. This also shows the hint of common sense because a woman and a little girl hugging together are most likely to be a mother and a daughter, which is hard to draw only from the picture.